

# High Gain Quadruple-Cascode GaN Low-Noise Amplifier for Ku-Band Satellite Applications

Anwar Jarndal

*Electrical Engineering Department  
University of Sharjah  
Sharjah, United Arab Emirates  
ajarndal@sharjah.ac.ae*

Husna Hamza

*Electrical Engineering Department  
University of Sharjah  
Sharjah, United Arab Emirates  
hhamza@sharjah.ac.ae*

**Abstract**—The future of satellite communication (SATCOM) is being revolutionized by constellations of medium Earth orbit (MEO) and low Earth orbit (LEO) satellites, delivering high-speed, low-latency connections with comprehensive global coverage. A critical requirement for low-noise amplifiers (LNAs) in these advanced satellite systems is the ability to maintain low noise levels while achieving high gain. This challenge is particularly pronounced at Kurz (Ku)-band microwave frequencies and above. This study explores the development of gallium nitride (GaN) high electron mobility transistor (HEMT) LNAs in innovative configurations—cascode, triple-cascode, and quadruple-cascode—tailored specifically for Ku-band satellite applications. Employing Keysight ADS design software, the LNAs are carefully designed, with their matching circuits optimized to enhance overall performance. All three LNAs demonstrate comparable noise performance, with a noise figure (NF) of approximately 2.2 dB at 13 GHz. However, the quadruple-cascode LNA stands out, achieving a remarkable gain of 37 dB at the same frequency, compared to 15.9 dB for the cascode and 25 dB for the triple-cascode configurations. The impressive gain of the quadruple-cascode LNA, i.e., more than double that of the cascode LNA, highlights its potential as a highly effective topology for microwave and millimeter-wave LNAs. The advancement paves the way for enhanced satellite communication capabilities.

**Keywords**—Gallium nitride high electron mobility transistor, Ku-band, low noise amplifiers, noise figure, satellite communications

## I. INTRODUCTION

A highly dynamic and robust low-noise amplifier (LNA) is an essential component of microwave receiving systems used in navigation, defense, and commercial communication due to the weak signal quality at the receiver input [1]-[3]. The current Internet of Things (IoT) networks enable the connection of hundreds of millions of devices globally, facilitating a wide range of practical applications in healthcare, agriculture, and risk detection and alarm systems. However, remote locations, i.e., deserts, oceans, forests, and the polar regions, remain underserved by these services. To address this gap and achieve the desired global coverage regardless of topography, future sixth-generation (6G) networks aim to integrate satellites into traditional IoT frameworks, giving rise to a new industry known as satellite IoT. Among the various types of satellites, small satellites have garnered significant research interest for this integration due to their low orbital altitudes, cost-effective manufacturing and launch processes, and minimal path degradation losses.

The space industry is increasingly focused on satellite communication due to the rapid advancements in low Earth orbit (LEO) satellite technology. Before signal processing, it is essential to amplify the signal while preserving its fidelity,

necessitating minimal added noise during amplification. Consequently, high gain and low noise figure (NF) are critical characteristics of an effective LNA. A significant challenge in LNA design lies in achieving an optimal trade-off between maximum gain, low NF, and low power consumption.

Historically, indium phosphide (InP) and gallium arsenide (GaAs)-based high-electron-mobility transistors (HEMTs) have been favored over silicon MOSFETs for very low-noise microwave receiver applications. However, due to their ability to handle large breakdown fields, gallium nitride (GaN) HEMTs have also been explored for low-noise and high-linearity applications. GaN HEMT technology offers excellent power and low-noise performance, making it a compelling choice for high-performance receivers [4]-[7]. The superior power handling capacity of GaN HEMTs is attributed to their wide bandgap of 3.4 eV, high breakdown voltage, and high saturation velocity. In addition to high power and low noise operation, GaN HEMTs exhibit remarkable overdrive capability and durability. Their high breakdown voltage allows for the elimination of additional RF limiting circuitry for input power handling in the LNA frontend, resulting in an overall reduction in system noise, size, and weight. This improved trade-off between performance and cost renders GaN HEMT-based receivers particularly attractive for satellite-based secure communication systems [8].

Several GaN HEMT LNA designs have been reported in the literature for Kurz (Ku)-band applications. In [9], a 150 nm GaN on silicon carbide (SiC) HEMT is utilized to design a Ku-band LNA, achieving a gain of 25 dB and a NF of 2.5 dB. A two-stage LNA designed in [10] employed 100 nm GaN HEMT technology, resulting in a gain of 18 dB and a NF of less than 3.5 dB. Additionally, a three-stage Ku-band LNA is presented in [11], where the HEMTs in all stages featured a gate length of 0.25  $\mu\text{m}$ . The first two stages used  $2\times 50\ \mu\text{m}$  HEMTs, while the final stage employed an  $8\times 60\ \mu\text{m}$  HEMT. The design achieved a NF of 1.9 dB and a gain of 19.8 dB. In [12], another Ku-band GaN HEMT LNA is reported, which attained a gain of 18 dB and a NF of 2.4 dB. Furthermore, a Ku-band LNA utilizing 250 nm GaN HEMT technology is developed in [13], achieving a NF of 1.85 dB and a gain of 20 dB. These studies highlight the need for a design approach aimed at achieving higher gain while maintaining low noise levels at Ku-band frequencies.

Recent research indicates a growing interest in LNA design. Various techniques are being employed to enhance LNA performance. These include optimizing circuit linkage with transistors and increasing the number of stages to boost gain. Common-emitter designs with inductive degeneration

and input inductors in the initial stage are also used to improve noise reduction and signal amplification. The common gate stage serves as the first stage of the amplifier. It matches input signals across a broad frequency range. This ensures efficient signal transfer from the input source and proper impedance matching. The common source stage functions as the second stage of the amplifier. Its primary role is to deliver substantial gain. Together, these two stages contribute to high gain and well-matched input, enhancing overall amplifier performance. This architecture, known as cascode, is utilized in this paper. The objective of this work is to develop a low-noise, high-gain Ku-band GaN amplifier designed for integration into the receiver front end.

The remainder of this paper is structured as follows. Section II details the GaN HEMT technology employed in this study and outlines the simulation framework. Section III describes the three LNA designs and the topologies utilized, including cascode, triple-cascode, and quadruple-cascode. Section IV presents the results in terms of gain, input/output matching, NF, and stability within the targeted frequency range. Finally, Section V offers conclusions that compare the performance of the three different topologies.

## II. DEVICE STRUCTURE AND MODELING FRAMEWORK

The GaN HEMT device, featuring a gate length of 0.25  $\mu\text{m}$  and a gate width of  $8 \times 50 \mu\text{m}$ , is modeled as reported in [14]. The S-parameters and noise parameters of this model are verified and found to be consistent under both cold ( $V_{GS} = -4 \text{ V}$ ,  $V_{DS} = 0 \text{ V}$ ) and active ( $V_{GS} = -2.72 \text{ V}$ , and  $V_{DS} = 10 \text{ V}$ ) bias conditions, as depicted in Fig. 1. The GaN HEMT model is implemented in Keysight ADS software and used for the design of the LNAs.

Under the same active bias conditions of  $V_{GS} = -2.72 \text{ V}$  and  $V_{DS} = 10 \text{ V}$ , noise modeling of the  $8 \times 50 \mu\text{m}$  gate width device is conducted. Fig. 2 illustrates the simulated and measured noise metrics, including the minimum NF ( $NF_{\min}$ ), equivalent noise resistance ( $R_n$ ), and optimum noise reflection coefficient ( $\Gamma_{\text{opt}}$ ). The results demonstrate a strong correlation between the measured and simulated data.

## III. LNA DESIGN CRITERION

The main design criteria for LNA design include stability, high gain, and low NF. In LNA design, maximum gain of  $S_{21}$  and minimum reflection coefficients for  $S_{11}$  and  $S_{22}$  can be

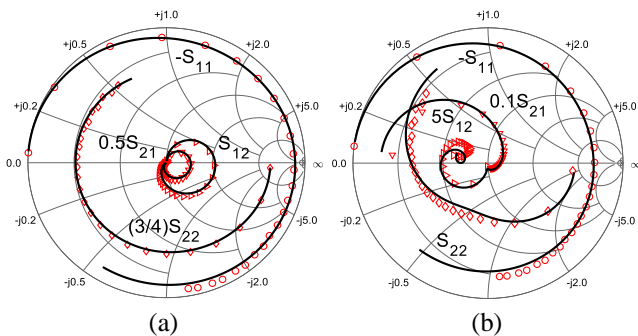


Fig. 1. Measured and simulated, i.e., symbols and lines, respectively, S-parameters at (a) off state ( $V_{GS} = -4 \text{ V}$ ,  $V_{DS} = 0 \text{ V}$ ) and (b) active bias ( $V_{GS} = -2.7 \text{ V}$ ,  $V_{DS} = 10 \text{ V}$ ) for a  $8 \times 50\text{-}\mu\text{m}$  gate width GaN HEMT up to 40 GHz [14].

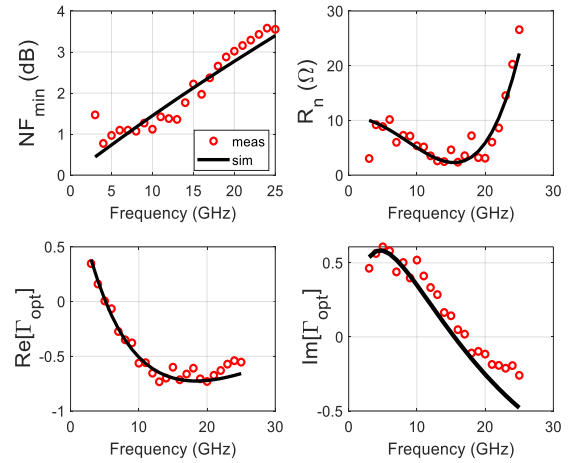


Fig. 2. Measured and simulated, i.e., circles and line, respectively, noise metrics of minimum noise figure, noise resistance and gamma optimum under active bias condition for  $8 \times 50 \mu\text{m}$  GaN HEMT [14].

achieved by fine-tuning the input and matching components. The input side of the LNA must be optimized for effective noise and power performance. Since the optimal points for noise and power do not coincide, it is essential to find the best compromise between these two factors. Ideal input and output reflection coefficients should be less than -10 dB to ensure good matching. Rollett's condition, i.e., K- $\Delta$  test, is employed to verify the stability of the LNA, as expressed in [15]:

$$\text{Stability Factor } K = \frac{(1 - (|S_{11}|^2 - |S_{22}|^2 + |\Delta|^2))}{2|S_{21}||S_{12}|} \geq 1, \quad (1)$$

$$\text{Delta } |\Delta| = |S_{11}S_{22} - S_{12}S_{21}| < 1. \quad (2)$$

To achieve unconditional stability, the delta factor ( $|\Delta|$ ) must be less than 1, while the stability factor ( $K$ ) should be greater than 1. The NF of the LNA represents its noise performance; a higher NF indicates greater signal degradation. Therefore, a lower NF should be the target when designing the LNA within the desired frequency range. The NF of the LNA is expressed as follows:

$$NF = NF_{\min} + R_n / G_s (Y_s - Y_{\text{opt}})^2 \quad (3)$$

where  $NF_{\min}$  represents the minimum NF that can be achieved by the LNA under optimal noise matching conditions. Moreover,  $R_n$  is the noise resistance, and  $G_s$  indicates the source conductance. It is evident that the NF of the LNA is influenced by the source termination ( $Y_s$ ), which must match the optimal noise impedance ( $Y_{\text{opt}}$ ) to attain  $NF_{\min}$ .

## IV. LNA DESIGN AND RESULTS

### A. Cascode LNA Design

The cascode LNA consists of two stages: a common-source stage feeding into a common-gate stage. Compared to a single-stage amplifier, the cascode amplifier offers enhanced shielding between the input and output, higher input impedance, greater output impedance, and a wider bandwidth. The increased output impedance isolation capability of the cascode LNA contributes to improved gain relative to the single-stage LNA. Additionally, reverse isolation is enhanced in the cascode structure, as the common-gate transistor helps suppress the Miller capacitance of the common-source transistor [16]. The designed cascode LNA operating at 13

GHz is demonstrated in Fig. 3, with a gate voltage of  $-2.72$  V and a drain voltage of  $10$  V.

The lumped components are optimized to achieve the best possible NF and gain. Input matching is accomplished by tuning the components  $C_1$ ,  $C_{in}$  and  $L_g$ . Interstage matching is achieved by adjusting the components  $L_4$  and  $C_3$ , which connect the common-source and common-gate stages. The source degeneration inductor ( $L_{s1}$ ) resonates with the parasitic capacitance at the output of the common-gate stage, thereby reducing the NF of the cascode amplifier. Fine-tuning of the source degeneration inductor is performed to mitigate the effects of parasitic capacitance at  $13$  GHz. Output matching is accomplished by carefully adjusting the series combination of  $R_1$  and  $C_4$ , which are added in shunt. The cascode LNA achieves a gain of  $15.9$  dB at  $13$  GHz and a NF of  $2.2$  dB, as shown in Fig. 4.

### B. Triple-Cascode LNA Design

In the triple-cascode LNA configuration, a single common-source stage is connected to two common-gate stages. This design results in a triple-cascode LNA featuring one common-source transistor and two common-gate transistors. The  $13$  GHz triple-cascode LNA is illustrated in Fig. 5.

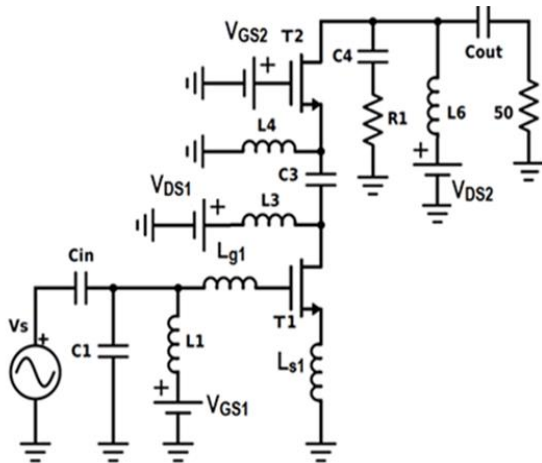


Fig. 3. Schematic circuit of the cascode low-noise amplifier.

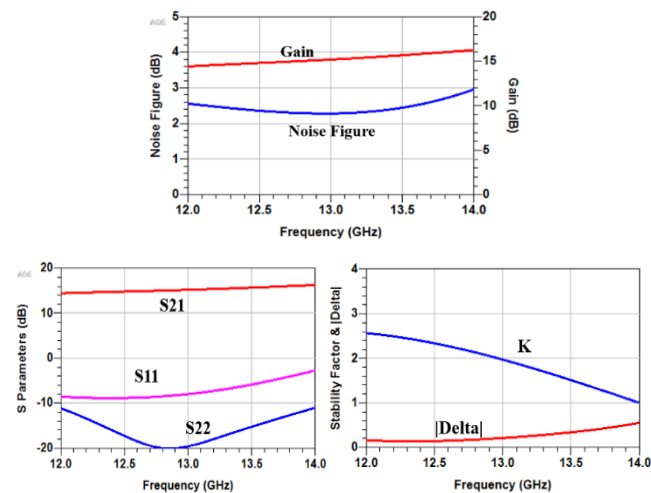


Fig. 4. Cascode low-noise amplifier: noise figure, gain, S-parameters and stability factors at  $12$ - $14$  GHz Ku-band frequencies.

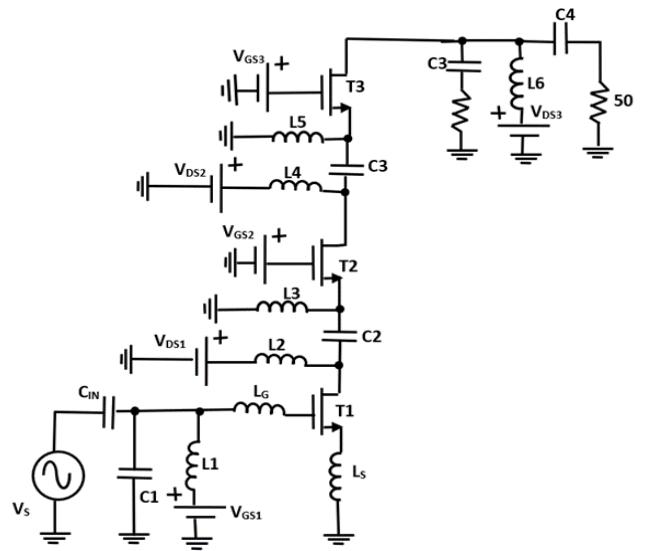


Fig. 5. Schematic circuit of the triple-cascode low-noise amplifier.

According to Fig. 6, the triple-cascode LNA achieves a gain of  $25$  dB and a NF of  $2.2$  dB. Compared to the cascode LNA, the triple-cascode LNA attains a larger gain, which can be attributed to the additional common-gate stage. The similar NF of the triple-cascode LNA, relative to that of the cascode LNA, is due to the fact that the NF of a cascaded system is primarily determined by the first stage, which is the common-source stage in this configuration.

### C. Quadruple-Cascode LNA Design

The quadruple-cascode LNA, illustrated in Fig. 7, consists of a single common-source stage followed by three common-gate stages. As shown in Fig. 8, the quadruple-cascode LNA achieves a gain of  $37$  dB and a NF of  $2.2$  dB. This configuration demonstrates a higher gain than the other two LNA designs while maintaining comparable noise performance. The increase in gain is attributed to the additional common-gate stage at the output, while the similar noise performance is due to the consistent input stage.

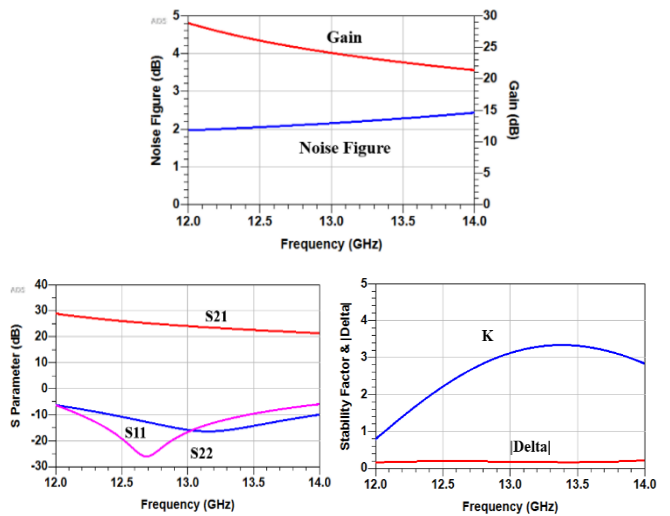


Fig. 6. Triple-cascode low noise amplifier: noise figure, gain, S-parameters and stability factors at  $12$ - $14$  GHz Ku-band frequencies.

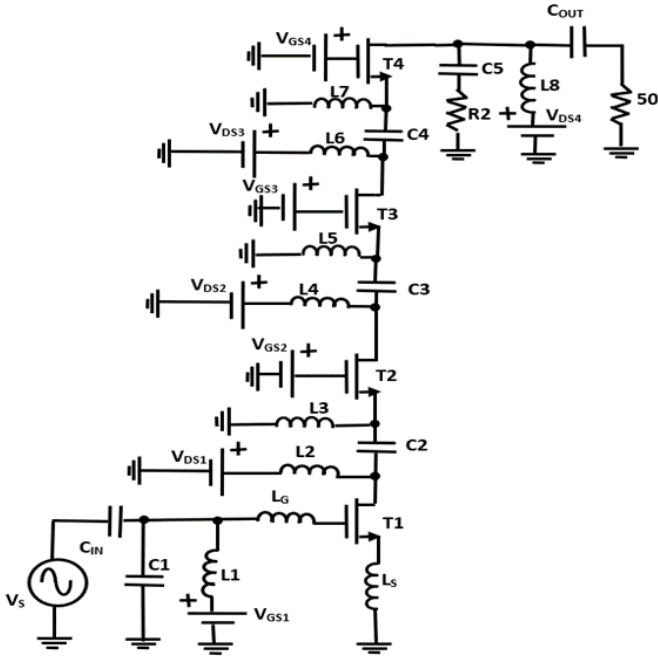


Fig. 7. Schematic circuit of the quadruple-cascode low-noise amplifier.

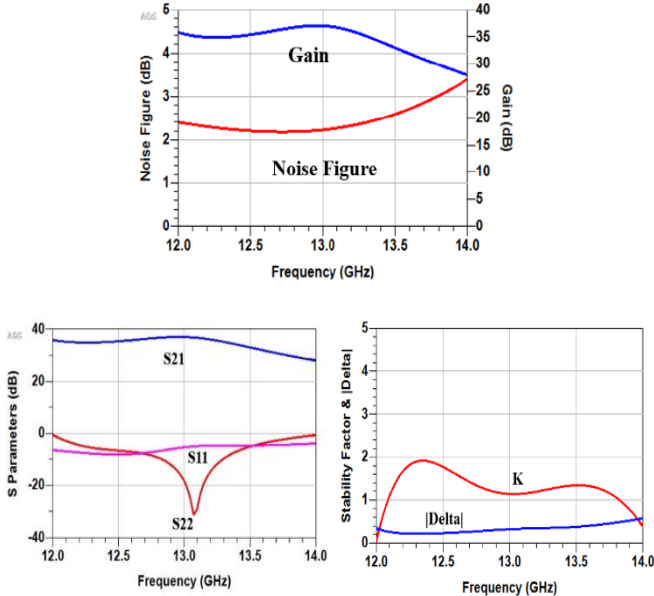


Fig. 8. Quadruple-cascode low-noise amplifier noise figure, gain, S-parameters and stability factors at 12-14 GHz Ku-band frequencies.

All results are presented in Table I for comprehensive comparison. Further optimization of the GaN HEMT at the device level presents an opportunity to achieve an even lower NF. The inclusion of an additional stage significantly enhances circuit-level performance. The findings demonstrate that the gain of the LNA can be effectively increased by adding a common-gate stage, while maintaining the NF of the amplifier. Notably, in the quadruple-cascode configuration, the gain of the LNA is 130% higher than that of the cascode LNA, underscoring the advantages of this design.

The performance of the presented quadruple-cascode LNA is evaluated against the most recent published work in Table II. The results demonstrate a significant improvement in gain compared to previously reported designs. The enhancement is made possible by the quadruple configuration, which preserves

the noise performance characteristic of the cascaded architecture. Furthermore, the performance of the quadruple-cascode LNA can be further enhanced by optimizing the HEMT to achieve a better NF. It is important to note that this improvement in gain comes at the expense of an increased number of HEMTs.

Table I: Gain and Noise Figure of Cascode Topologies of the Low-Noise Amplifier

Cascode LNA	Gain (dB)	Noise Figure (dB)
Cascode LNA	15.9	2.2
Triple-Cascode LNA	25	2.2
Quadruple-Cascode LNA	37	2.2

Table II: Comparison of Obtained Results for the Quadruple-Cascode Low-Noise Amplifier with State-of-the-Art Solutions.

Ref.	Freq (Ghz)	Gain (dB)	NF (dB)	Gate width (nm)	Gate Length (nm)	No. of HEMT
[17]	13	11.5	0.98	400	250	1
[18]	18	16	2.2	200	100	4
[19]	15	21.3	1.7	200	200	1
This work	13	37	2.2	400	250	4

## V. CONCLUSION

This work presents the design of GaN HEMT LNAs for Ku-band satellite applications in three distinct configurations: cascode, triple-cascode, and quadruple-cascode. Within the desired operating frequency range, the quadruple-cascode LNA achieves an impressive maximum gain of 37 dB while maintaining a comparable NF of 2.2 dB, consistent with the performance of both the cascode and triple-cascode designs. Notably, the gain improves more than twofold from the cascode to the quadruple-cascode configuration, without any adverse impact on the NF. These results affirm the suitability of the quadruple-cascode LNA for high-performance satellite receiver front ends, offering significant gains alongside low noise characteristics essential for advanced communication systems.

## ACKNOWLEDGMENT

The authors gratefully acknowledge the support from the University of Sharjah, Sharjah, United Arab Emirates.

## REFERENCES

- [1] X. Yan, J. Zhang, S. -P. Gao and Y. Guo, "Beyond the Bandwidth Limit: A Tutorial on Low-Noise Amplifier Circuits for Advanced Systems Based on III-V Process," in *IEEE Transactions on Circuits and Systems II: Express Briefs*, vol. 71, no. 3, pp. 1644-1649, March 2024, doi: 10.1109/TCSII.2023.3338812
- [2] N. C. Miller *et al.*, "A Survey of GaN HEMT Technologies for Millimeter-Wave Low Noise Applications," in *IEEE Journal of Microwaves*, vol. 3, no. 4, pp. 1134-1146, Oct. 2023, doi: 10.1109/JMW.2023.3313111
- [3] M. Yaghoobi, M. Yavari, M. H. Kashani, H. Ghafoorifard, and S. Mirabbasi, "A 55-64GHz low-power small-area LNA in 65-nm CMOS with 3.8-dB average NF and 12.8-dB power gain," in *IEEE Microw. Wireless Compon. Lett.*, vol. 29, no. 2, pp. 128-130, Feb 2019.
- [4] X. Liu *et al.*, "0.18 dB Low-Noise Figure at 10 GHz for GaN MIS-HEMT With Plasma-Enhanced Atomic Layer Deposition SiN Layer," in *IEEE Electron Device Letters*, vol. 44, no. 7, pp. 1080-1083, July 2023, doi: 10.1109/LED.2023.3282621

- [5] J. Zhou *et al.*, "RF p-GaN HEMT With 0.9-dB Noise Figure and 12.8-dB Associated Gain for LNA Applications," in *IEEE Electron Device Letters*, vol. 44, no. 9, pp. 1412-1415, Sept. 2023, doi: 10.1109/LED.2023.3294696
- [6] X. Tong, P. Zheng and L. Zhang, "Low-Noise Amplifiers Using 100-nm Gate Length GaN-on-Silicon Process in W-Band," in *IEEE Microwave and Wireless Components Letters*, vol. 30, no. 10, pp. 957-960, Oct. 2020, doi: 10.1109/LMWC.2020.3019816
- [7] C. -J. Yu, C. -W. Hsu, M. -C. Wu, W. -C. Hsu, C. -Y. Chuang and J. -Z. Liu, "Improved DC and RF Performance of Novel MIS p-GaN-Gated HEMTs by Gate-All-Around Structure," in *IEEE Electron Device Letters*, vol. 41, no. 5, pp. 673-676, May 2020, doi: 10.1109/LED.2020.2980584.
- [8] Anwar Jarndal and Husna Hamza K "On GaN Low Noise Amplifier: Device Modelling and Circuit Design" *International Journal on Communications Antenna and Propagation*, Vol 13, No 1, February 2023.
- [9] P. Gupta, M. Imran and M. Mishra, "GaN HEMT based Ku band LNA and SPDT Switch for Transmit-Receive application," 2022 IEEE International Conference on Emerging Electronics (ICEE), Bangalore, India, 2022, pp. 1-5, doi: 10.1109/ICEE56203.2022.10117990.
- [10] Q. Lin, H. Wu, Y. Chen, L. Hu, S. Chen and X. Zhang, "A Compact Ultra-broadband GaN MMIC T/R Front-End Module," 2020 IEEE/MTT-S International Microwave Symposium (IMS), Los Angeles, CA, USA, 2020, pp. 1231-1234, doi: 10.1109/IMS30576.2020.9223795.
- [11] Suijker, E.M. & Rodenburg, M. & Hoogland, J.A. & Heijningen, M. & Seelmann, M. & Quay, Rüdiger & Brückner, Peter & Vliet, F.E.. (2009). Robust AlGaIn/GaN low noise amplifier MMICs for C-, Ku- and Ka-band space applications. *IEEE Transactions on Electron Devices*-1 - 4. 10.1109/csics.2009.5315640.
- [12] F. Guo and Z. Yao, "Design of a Ku-band AlGaIn/GaN low noise amplifier," *Proceedings of 2014 3rd Asia-Pacific Conference on Antennas and Propagation*, Harbin, China, 2014, pp. 1406-1408, doi: 10.1109/APCAP.2014.6992789.
- [13] D. Resca *et al.*, "A robust Ku-band low noise amplifier using an industrial 0.25- $\mu$ m AlGaIn/GaN on SiC process," 2013 European Microwave Conference, Nuremberg, Germany, 2013, pp. 1467-1470, doi: 10.23919/EuMC.2013.6686945.
- [14] Jarndal, A, Hussein, A, Crupi, G, Caddemi, A. Reliable noise modeling of GaN HEMTs for designing low-noise amplifiers. *Int J Numer Model.* 2020; 33:e2585. <https://doi.org/10.1002/jnm.2585>
- [15] David M. Pozar (2012). *Microwave Engineering* 4th Edition. In John Wiley & Sons Inc.
- [16] Kalantari, Fatemeh, Nasser Masoumi, and Fatemeh Sadat Saadati. "A low power 90 nm LNA with an optimized spiral inductor model for WiMax front end." *2006 49th IEEE International Midwest Symposium on Circuits and Systems*. Vol. 1. IEEE, 2006.
- [17] H. Hamza and A. Jarndal, "A Sub-1dB Noise Figure Ku Band GaN Low Noise Amplifier for Space Applications," *2023 International Conference on Microelectronics (ICM)*, Abu Dhabi, United Arab Emirates, 2023, pp. 168-171, doi: 10.1109/ICM60448.2023.10378929
- [18] Tong, Xiaodong, *et al.* "An 18–56-GHz wideband GaN low-noise amplifier with 2.2–4.4-dB noise figure." *IEEE Microwave and Wireless Components Letters* 30.12 (2020): 1153-1156.
- [19] Han, Seong-Hee, and Dong-Wook Kim. "Robust Ku-Band GaN Low-Noise Amplifier MMIC." *Journal of Electromagnetic Engineering and Science* 24.2 (2024): 170-177.